

Electronic Supplementary Information (ESI)

Fabrication of sandwich structural electrode for high-performance lithium-sulfur battery

Bing Ding,^a Guiyin Xu,^a Laifa Shen,^a Ping Nie,^a Pengfei Hu,^b Hui Dou,^a and Xiaogang Zhang^{a*}

^aCollege of Material Science and Engineering and Key Laboratory for Intelligent Nano Materials and Devices of Ministry of Education, Nanjing University of Aeronautics and Astronautics, Nanjing 210016, P. R. China. Fax: 86-02552112626; Tel: 86-02552112918; E-mail: azhang@163.com

^bLaboratory for Microstructures, Shanghai University, Shanghai 200444, P. R. China

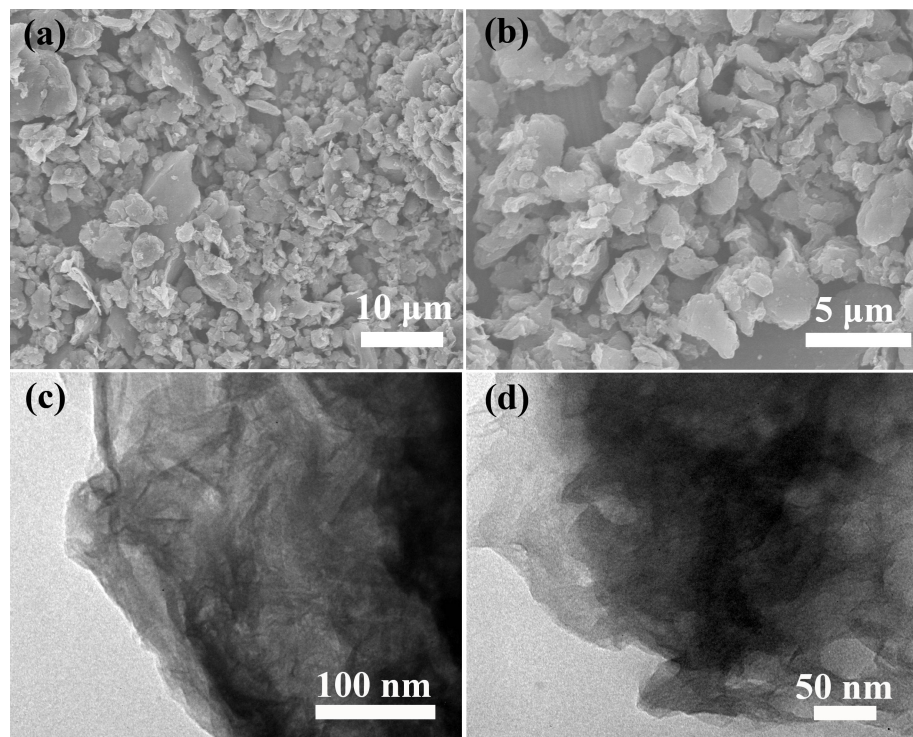


Fig. S1 (a, b) SEM images and (c, d) TEM images of Graphene/S composite.



Fig. S2 STEM image of Graphene/TiO₂/S nanocomposite.

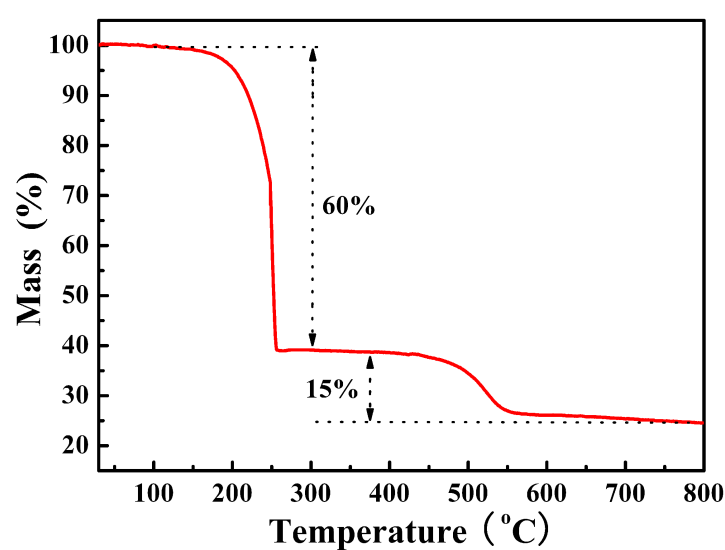


Fig. S3 TG curves of Graphene/TiO₂/S nanocomposite.

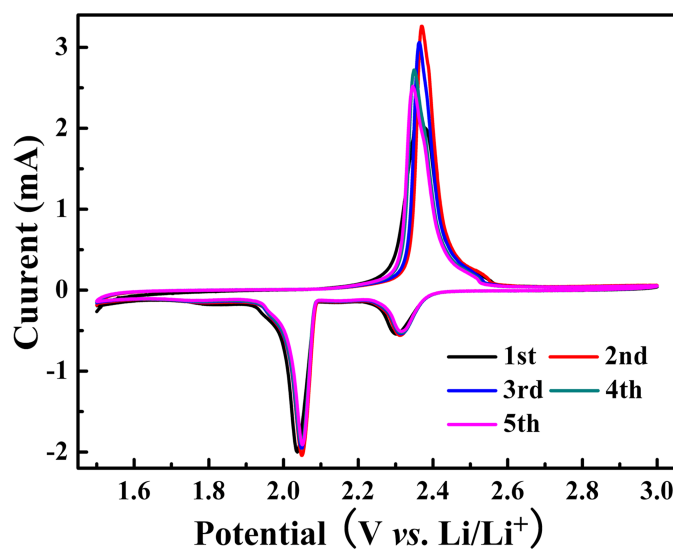


Fig. S4 CV curves of Gaphene/S electrode at a scaning rate of 0.2 mV s^{-1} .

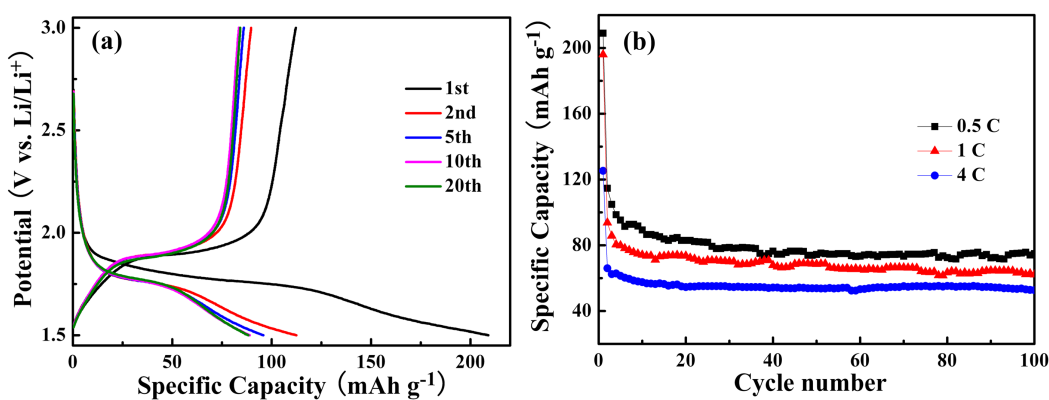


Fig. S5 Electrochemical behaviors of Graphene/TiO₂ electrode: (a) Galvanostatic charge-discharge profiles at a current rate of 0.5 C ($1\text{C}=170 \text{ mA g}^{-1}$). (b) Cycling performance at different current densities. (All measurements were conducted in the same potential window and electrolyte with that of Graphene/TiO₂/S electrode.)

As an electrochemically active host, the cycling stability and rapid ionic/electronic transport of Graphene/TiO₂ electrode is critical to the electrochemical performances of Graphene/TiO₂/S. As shown in Fig. S4, the Graphene/TiO₂ electrode exhibits

typical electrochemical behaviors of anatase TiO_2 . Fig. S3a shows the galvanostatic charge/discharge profiles at a current rate of 0.5 C. The two voltage plateaus appear at approximately 1.7 and 1.9 V are related to the phase transition between the tetragonal and orthorhombic phases with Li insertion into anatase TiO_2 .^{1,2} The Graphene/ TiO_2 electrode shows a first discharge capacity of 209 mAh g^{-1} and a subsequent charge capacity of 114 mAh g^{-1} . The high irreversible capacity loss could be contributed to the formation of an inactive solid/electrolyte interphase (SEI) on the surface of the TiO_2 nanocrystal.^{3,4} In the 5th cycle, the discharge capacity decreased to 95 mAh g^{-1} with a corresponding charge capacity of 89 mA h g^{-1} , leading to a much higher Coulombic efficiency of 94%. Compared with previous reports,^{1,2,5-7} the Graphene/ TiO_2 electrode shows lower specific capacities. This may due to two reasons: (1) as shown in the TGA curve (Fig. S1), the content of active TiO_2 in the Graphene/ TiO_2 (62.5 wt%) is relatively lower. (2) The potential window (1.5~3 V) is much narrower than that in previous reports. However, as depicted in Fig. S4b, the Graphene/ TiO_2 electrode exhibits excellent cycling stability and rate performance. For the Graphene/ TiO_2 electrode, the mesoporous and sandwich nanostructure could favor rapid diffusion of the electrolyte and lead to shortened diffusion path. Meanwhile, the highly conductive graphene layer act as a continuous conductor to facilitate easier electron transport.

Table S1 Comparison of electrochemical performances of sandwich structural Graphene/TiO₂/S electrode with the results of similar reports

Graphene-based hosts	Cycling Performance	Reference
GO with epoxy and hydroxyl groups	954 mA h g ⁻¹ /0.1 C/50th cycle	S8
Sulfur assisted exfoliated graphene	615 mA h g ⁻¹ /1 C/100th cycle	S9
PEG modified GO-carbon	520 mA h g ⁻¹ /0.2 C/100th cycle	S10
Graphene reduced by hydrazine	819 mA h g ⁻¹ /0.05 C/100th cycle	S11
Nafion coated Graphene	662 mAh g ⁻¹ /1 C/100th cycle	S12
Hydrofluoric acid treated graphene	800 mA h g ⁻¹ /0.1 C/50th cycle	S13
KOH activated graphene	829 mA h g ⁻¹ /0.1 C/50 cycle	S14
Sandwich structural Graphene/TiO ₂	765 mA h g ⁻¹ /0.5 C/ 100th cycle	this work
	737 mAh g ⁻¹ /0.5 C/ 100th cycle	

References:

- S1. J.S. Chen, Y.L. Tan, C.M. Li, Y.L. Cheah, D. Luan, S. Madhavi, F.Y.C. Boey, L.A. Archer, X.W. Lou, *J. Am. Chem. Soc.*, 2010, **132**, 6124.
- S2. D.H. Wang, D. Choi, J. Li, Z.G. Yang, Z.M. Nie, R. Kou, D.H. Hu, C.M. Wang, L.V. Saraf, J.G. Zhang, I.A. Aksay, J. Liu, *ACS Nano*, 2009, **3**, 907.
- S3. Z.X. Yang, G.D. Du, Q. Meng, Z.P. Guo, X.B. Yu, Z.X. Chen, T.L. Guo, R. Zeng, *J. Mater. Chem.*, 2012, **22**, 5848-5854.
- S4. D. Deng, M.G. Kim, J.Y. Lee, J. Cho, *Energy Environ. Sci.*, 2009, **2**, 818–837.
- S5. S.J. Ding, J.S. Chen, D.L. Luan, F.Y.C. Boey, S. Madhavi, X.W. Lou, *Chem. Commun.*, 2011, **47**, 5780.
- S6. N. Li, G. Liu, C. Zhen, F. Li, L.L. Zhang, H.M. Cheng, *Adv. Funct. Mater.*, 2011, **21**, 1717.
- S7. S.B. Yang, X.L. Feng, K. Muller, *Adv. Mater.*, 2011, **23**, 3575.
- S8. L. W. Ji, M. M. Rao, H. M. Zheng, L. Zhang, Y. C. Li, W. H. Duan, J. H. Guo, E. J. Cairns and Y. G. Zhang, *J. Am. Chem. Soc.*, 2011, **133**, 18522.
- S9. T. Q. Lin, Y. F. Tang, Y. M. Wang, H. Bi, Z. Q. Liu, F. Q. Huang, X. M. Xie and M. H. Jiang, *Energ Environ. Sci.*, 2013, **6**, 1283.
- S10. H. L. Wang, Y. Yang, Y. Y. Liang, J. T. Robinson, Y. G. Li, A. Jackson, Y. Cui and H. J. Dai, *Nano Lett.*, 2011, **11**, 2644.
- S11. B. Wang, K. F. Li, D. W. Su, H. J. Ahn and G. X. Wang, *Chem. Asian J.*, 2012, **7**, 1637.
- S12. Y. L. Cao, X. L. Li, I. A. Aksay, J. Lemmon, Z. M. Nie, Z. G. Yang and J. Liu, *Phys. Chem. Chem. Phys.*, 2011, **13**, 7660.
- S13. M. S. Park, J. S. Yu, K. J. Kim, G. Jeong, J. H. Kim, Y. N. Jo, U. Hwang, S. Kang, T. Woo and Y. J. Kim, *Phys. Chem. Chem. Phys.*, 2012, **14**, 6796.
- S14. B. Ding, C. Z. Yuan, L. F. Shen, G. Y. Xu, P. Nie, Q. X. Lai and X. G. Zhang, *J. Mater. Chem. A*, 2012, **1**, 1096.